

Matthew J. Richter, John H. Lacy, Daniel T. Jaffe, Douglas J. Mar, John Goertz, William M. Moller, Shadrian Strong and Thomas K. Greathouse, "Development and future use of the echelon-cross-echelle spectrograph on SOFIA", Proc. SPIE 6269, 62691H (2006).

Copyright 2006 Society of Photo Optical Instrumentation Engineers. One print or electronic copy may be made for personal use only. Systematic electronic or print reproduction and distribution, duplication of any material in this paper for a fee or for commercial purposes, or modification of the content of the paper are prohibited.

<http://dx.doi.org/10.1117/12.670559>

Development and future use of the echelon-cross-echelle spectrograph on SOFIA

Matthew J. Richter,^a John H. Lacy,^b
Daniel T. Jaffe,^b Douglas J. Mar,^b John Goertz,^b William M. Moller,^b Shadrian Strong,^b and
Thomas K. Greathouse^c

^aPhysics Dept - UC Davis, 1 Shields Ave, Davis, CA USA;

^bAstronomy Dept - UT Austin, 1 University Station C1400, Austin, TX USA;

^cLunar and Planetary Institute, 3600 Bay Area Blvd, Houston, TX, USA

ABSTRACT

The Echelon-cross-Echelle Spectrograph (EXES) will provide the Stratospheric Observatory for Infrared Astronomy (SOFIA) with high spectral resolution capabilities in the mid-infrared. EXES will have a maximum spectral resolving power of 100,000 along with lower resolution options (R=10,000; R=3000). EXES on SOFIA will provide sensitivity and spectral resolution never before available from an orbital or sub-orbital platform. Because of the wealth of molecular features in the EXES spectral range, 4.5 to 28.3 μm , and the dramatic reduction in telluric atmospheric interference provided by SOFIA, EXES will be particularly relevant for studies of the solar system, star formation and the interstellar medium. We report on the EXES design and current status, provide descriptions of observing modes and sensitivity estimates, discuss the calibration and likely data products, and describe the potential gains of incorporating a 1024×1024 , low-background, Si:As detector array.

Keywords: SOFIA, astronomical instruments, mid-IR, spectroscopy

1. INTRODUCTION

The portion of the electromagnetic spectrum from 4.5 to 28 μm , referred to here as the mid-infrared (MIR), contains a wealth of molecular transitions. In the context of astrophysics, these features predominantly arise in solids such as ices and in gaseous material.

While ice features are relatively broad (Figure 1), gas phase molecular features from objects within our Galaxy are usually quite narrow (<50 km/s with <10 km/s more typical). Gas-phase molecular absorption and emission are important diagnostics for objects within our solar system, for the study of star and planet formation, and for investigating the interstellar medium. By resolving individual transitions within a gas-phase ro-vibrational ladder, it becomes practical to derive physical parameters such as gas temperature and molecular abundances. The molecules in circumstellar and interstellar environments likely include the basic building blocks that lead to complex species important to life.

While much work in the MIR region of the spectrum can be done from the ground, the presence of molecules in our atmosphere prevents observations at many MIR wavelengths. The telluric atmosphere impacts observations in two ways; not only does it absorb photons from targets in space, it also contributes extra noise through the

Further author information: (Send correspondence to MJR)

MJR: E-mail: mjrichter@ucdavis.edu, Telephone: 1 530 752 2226

JHL: E-mail: lacy@astro.as.utexas.edu, Telephone: 1 512 471 1469

DTJ: E-mail: dtj@astro.as.utexas.edu, Telephone: 1 512 471 3425

DJM: E-mail: djmar@astro.as.utexas.edu, Telephone: 1 512 471 6332

JG: E-mail: jgoertz@astro.as.utexas.edu, Telephone: 1 432 471 5400

WMM: E-mail: billm@shrub.as.utexas.edu, Telephone: 1 512 471 1472

SS: E-mail: sholmes@astro.as.utexas.edu, Telephone: 1 512 471 3466

TKG: E-mail: greathouse@lpi.usra.edu, Telephone: 1 281 486 2114

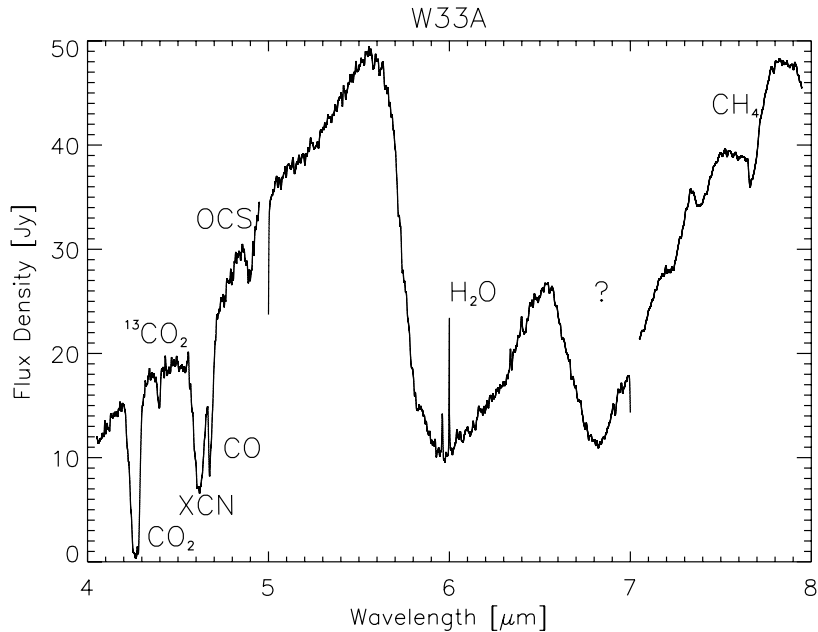


Figure 1. ISO data for W33A showing ice features between 4 and 8 microns.¹ Numerous species are seen and substructure within the bands indicate minor constituents. The spike at 6 μm comes from our reprocessing of the ISO data for this figure and is not real.

emission of thermal photons. Reducing the path-length light follows through the telluric atmosphere, (by observing from high altitude) helps improve the quality of MIR observations. SOFIA, the Stratospheric Observatory for Infrared Astronomy, will provide an observing platform above much of the telluric atmosphere.

SOFIA is a 747 airplane equipped with a 2.5m aperture telescope. It will fly at altitudes as high as 45,000 feet. For recent summaries regarding SOFIA see Ref. 2 or Ref. 3. SOFIA will have a suite of imaging and spectroscopic instruments. Because SOFIA has the capability to carry large instruments, the observatory will provide observational opportunities unlike those possible from space or the ground.

Among the SOFIA first light instruments is EXES, the Echelon-cross-Echelle Spectrograph. EXES is a MIR spectrograph being designed and built as a PI-class SOFIA instrument at The University of Texas (PI: John Lacy). EXES is similar in design and capabilities to the ground-based instrument TEXES.⁴ The primary motivation for EXES is the study of gas-phase molecules, so high spectral resolution is imperative. Additional operating modes, including long slit moderate and low resolution spectroscopy, are available. In this paper, we will present the basic EXES design along with the status of various subsystems in Section 2 and describe how we envision observing with EXES on SOFIA in Section 3. In Section 4, we will discuss treatment of the data. In Section 5 we will present sample science projects for EXES as currently configured and describe the possible science gain if EXES incorporates a 1024×1024 detector array in Section 6.

2. EXES DESIGN AND CURRENT STATUS

EXES is a LHe-cooled instrument with three major optical subsystems, a MIR detector and electronics, associated mechanical/thermal packaging, instrument control systems and attending software, and support equipment. We will summarize the design and status of these various components below. For more insight into the details of the design, see Ref. 5 and Ref. 6.

The optics consist of three major subsystems: the foreoptics, the high dispersion echelon and its associated mirrors, and the cross-dispersion grating and its mirrors. The foreoptics include an ellipsoid to change the

incoming SOFIA f/20 beam to f/10 within EXES. The entrance window to the cryogenic volume doubles as a field lens to image the telescope pupil at a cold stop. The final element of the foreoptics includes a filter wheel followed closely by a decenter wheel and a slit wheel. The high dispersion area contains the echelon grating, a 4-inch by 40-inch monolithic grating blazed at R10.⁷ We use an off-axis paraboloid as the collimator and camera mirror for the echelon. The cross-dispersion area will have a diamond-machined echelle grating blazed for R2.4. In addition, we will be able to use the echelle as a retroreflector at lower angle, as an inefficient mirror in 0th order, and as a low dispersion grating by rotating past face-on to negative orders where it is blazed at R0.4.

The optics, with the exception of the cross-dispersion grating, are in hand. We tested individual components warm and found the foreoptics ellipsoid and the echelon paraboloid will be diffraction limited to 5 μm . Tests on the echelon grating suggest it is diffraction limited for $\lambda > 8 \mu\text{m}$ and satisfactory for $\lambda > 4 \mu\text{m}$. The optics support structure and its mechanisms are fully assembled and have been tested warm.

The baseline detector for EXES is a Raytheon 256 \times 256 Si:As array designed for low backgrounds. This array is the same type as operates in the IRAC instrument aboard the Spitzer Space Telescope.⁸ We have been using the array in TEXES and find that it performs well for high resolution spectroscopy. We purchased the electronics to run the array from Wallace Instruments and have been using it with minimal modifications since 2000.

In Section 6 we discuss the potential of using a 1024 \times 1024 pixel Si:As array in EXES.

The cryogenic dewar has been received from Precision Cryogenics. The G10 fiberglass supports are much more rigid than an earlier design incorporated in TEXES. This should help limit flexure during operations. We expect the LHe hold time to be more than two days. Hold time tests will be done in summer, 2006. Unfortunately, flanges on the vacuum container walls warped during welding. The outer walls will need to be remade with a modified flange design intended to reduce welding stresses. The handling cart for the completed instrument is complete and works well.

Control of instrument mechanisms has been tested with TEXES working at the NASA IRTF and Gemini-North. Motion from stepper motors passes through to the cryogenic volume using ferrofluidic feedthroughs and fiberglass shafts. We use 10 turn potentiometers coupled directly to the gears driving the ferrofluidics for position sensing. We use a PC running Labview to communicate with the stepper motor controllers. A limited number of low level commands were incorporated in the Labview program. The higher level software runs on the overall instrument control computer, a Linux machine running a combination of Tcl/tk and C, and incorporates substantial knowledge of the instrument to make observations easier to prepare.

Much of the instrument control, data acquisition, and data reduction software that will be used on EXES has been proven using TEXES.

3. EXES OPERATIONS AND PERFORMANCE

Because EXES is a PI-class instrument, members of the instrument team will always be present and will operate the instrument. General Investigators (GIs) using EXES on SOFIA will be expected to work with the instrument team to determine the feasibility of particular experiments and the best observing strategy for a given target. Detailed information regarding target acquisition will be the responsibility of the GIs.

EXES will have 5 standard operating modes while on the telescope: high, medium, and low resolution spectroscopy, source acquisition imaging, and pupil viewing. High-resolution spectroscopy uses all optical subsystems and results in cross-dispersed spectra with a limited slit length. Medium and low resolution spectroscopy do not involve the echelon grating or its collimator/camera mirror; in these modes the cross-dispersion grating is used as the sole disperser and a portion of a single order is recorded on the detector. Acquisition imaging uses the same optics as medium and low resolution spectroscopy with the slit in an open position and the cross-dispersion grating face-on. For pupil viewing, focal reducing optics immediately before the detector are adjusted to image the pupil on the detector. Each operating mode, when specified by the operator, indicates to the software where each relevant optic should be positioned based on a look-up table.

In high-resolution spectroscopic mode, the instrument operator will enter the desired central wavenumber to fully configure the instrument. At present time, motors move serially with software safety checks that require the

user to confirm motions. The software is designed to remove backlash and hysteresis in mechanisms, but we still find small corrections to the initial positioning are useful. Instrument configuration parameters such as slit width, length, and blocking filter depend on the wavenumber selected and the performance of the cross-dispersion grating at that wavenumber. The default slit width is roughly $1.5\lambda/D$ with a minimum width defined to give $R \approx 100,000$ without too much loss of light. We will maximize the slit length while preventing neighboring echelon spectral orders from overlapping. The blocking filter will be chosen to isolate the echelle order and prevent unwanted light from contaminating the spectrum. At short wavelengths it will be possible for the experimenter to choose between increased slit length or increased wavelength coverage depending on which order the cross-dispersion grating operates. Suggested integration times and array clocking patterns will also be set depending on the instrument configuration.

The amount of cross-dispersion is somewhat selectable depending on the needs of the experiment. In typical operation, the echelle cross-disperser will be used to provide slit lengths on order $5''$ with roughly 6-10 echelon orders falling on the detector simultaneously. This format results in instantaneous wavelength coverage of roughly 0.5%. For applications where larger wavelength coverage is essential, it will be possible to use the back side of the echelle grooves as a first-order grating with very low dispersion. The resulting cross-dispersed spectrum will have a very short slit, length comparable to the width, and roughly 25 echelon orders recorded by the detector simultaneously.

Once the instrument is configured, it will be necessary to acquire a spectrum to confirm the set-up. This spectrum can be of a gas cell where known constituent gases serve to identify the spectral region. The molecular transitions from the gas species will appear in emission as the gas cells are intended to reflect the beam back to the cold optics of the dewar. Alternatively, a sky emission spectrum can be used to verify the setup. Both gas cell and sky emission spectra are suitable for wavelength calibration across the entire array. Given performance on TEXES, we expect the solution to be valid to better than 0.5 km/s across the array.

Instrument configuration for the other modes is similar. For low and moderate resolution spectroscopy, the operator specifies the central wavenumber and the software provides a default configuration with the long slit, appropriate filter, and suggested array clocking patterns and integration times. Because the cross-dispersion and the detector size define the wavelength coverage, low and moderate resolution spectroscopy do not offer increased wavelength coverage (except for $\lambda > 10 \mu\text{m}$ where the echelon spectral orders are larger than the 256×256 detector). The lower spectral resolution modes do, however, offer much longer slits (e.g. $30''$). The imaging modes are intended to operate with as few modifications to the optical path as possible. We have seen that the TEXES source acquisition mode introduces a change in the optical path, and returning to the exact setup is impractical. While a basic difference between the TEXES and EXES design, namely use of a flip mirror with hard stops to select whether to use the echelon grating or not, may alleviate this problem, elements such as the slit and cross-dispersion grating will be required to move for full field imaging. Depending on EXES performance and the SOFIA pointing, it may be more efficient to find an object in spectroscopic mode than in EXES imaging.

We note that EXES is not intended to be a science camera. Performance estimates for the EXES high-resolution spectroscopic mode are presented in Figure 2. These estimates assume the observatory meets its requirement for image quality.

We expect observing with any SOFIA instrument will be highly scripted prior to departure. The need to file flight plans that return the observatory to its base with minimal wasted time requires following a well-thought-out plan. GIs will be responsible for prioritizing observations, planning integration times, and providing concrete methods for source acquisition. A typical EXES observing session on SOFIA will include initial wavelength setup prior to takeoff, confirmation of the optical/IR boresight registration, and observations of targets. As noted above, sky emission spectra or gas cell observations are suitable for wavelength calibration. Until we determine the level of flexure in EXES, we must allow for blackbody observations to properly flatfield the data. Depending on stability during takeoff, it may be necessary to fine-tune the instrument configuration once in the air. We hope that the optical/IR boresight will be consistent at least until the instrument is remounted on the telescope. If true, this will eliminate a potentially time-consuming calibration step from all but the first flight in an EXES flight series.

For each science project, it will be necessary to determine if telluric and flux standards are required. Asteroids are preferred for telluric standards at long wavelengths since they have essentially featureless continua over our

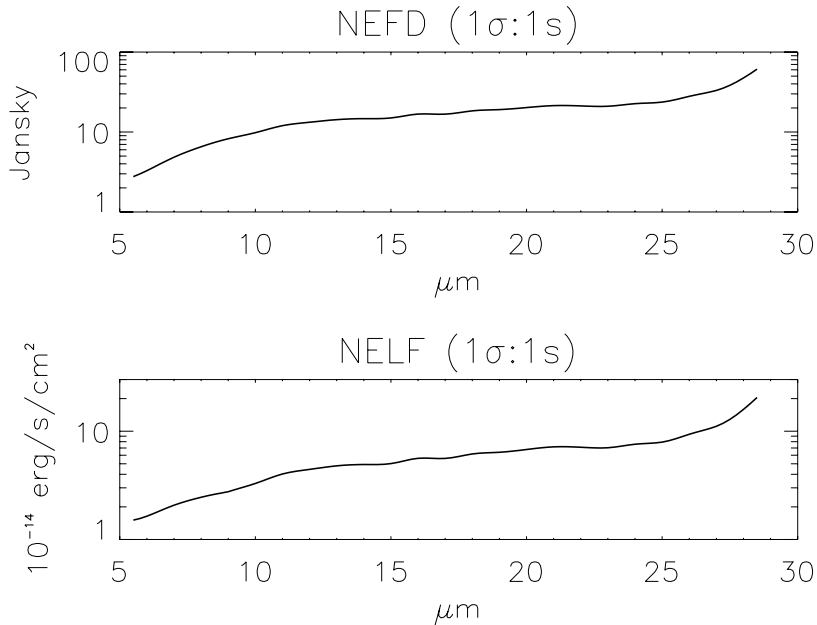


Figure 2. Estimated high-resolution sensitivity for EXES on SOFIA as a function of wavelength. The numbers given are 1σ for 1 second on-source for a continuum object (top) and an unresolved line (bottom). The estimates assume SOFIA image quality is diffraction-limited for $\lambda > 15 \mu\text{m}$ and that residual atmospheric transmission is 100%.

limited instantaneous wavelength coverage. At short wavelengths, hot stars with spectral type earlier than F have proven reliable telluric calibrators from the ground.

If mechanisms are sufficiently repeatable, we will be able to observe multiple wavelengths on a given target (flight leg) before switching to a separate target and repeating the wavelength settings as necessary. The best results may require observing multiple targets (flight legs) at a single wavelength before switching to a new setting. In either case we expect efficient use of time to force observations of multiple science projects on any single flight and forming a *de facto* EXES queue.

There will be two basic observing patterns with EXES: nodding and slit scanning. For all EXES observations, it will be necessary to remove background emission to view the target. For sources small compared to the slit length, we will move the telescope by a small amount to locate the target on a distinct portion of the slit. There will be some time lost during and after the move because of telescope settling and array readout time. For larger extended objects, it may be necessary to move the object completely off the slit to remove just the background emission. The penalty is a roughly square-root of two reduction in the SNR achieved for a given elapsed time. The short slit required to use the cross-dispersion grating in first order and record a large wavelength range necessitates nodding off the slit. In cases where a three dimensional (two spatial and 1 spectral) map is desired, the slit can be stepped across the target. Background emission is recorded, ideally, on both sides of the target. This mode is fairly efficient for acquiring this type of data, but works best for targets with strong emission in a distinct feature that can be used to align separate maps during data processing.

4. EXES DATA PROCESSING

EXES data processing will build upon our experience with the TEXES ground-based instrument.⁴ We have existing quick-look data acquisition tools and a near real-time data reduction pipeline. These programs are familiar to the EXES instrument team and will be run by them as part of the collaboration between instrument team members and SOFIA GIs. GIs using EXES will receive raw and reduced data as well as the processing software, but we expect most GIs to focus on their analysis efforts on the reduced data we send them. The

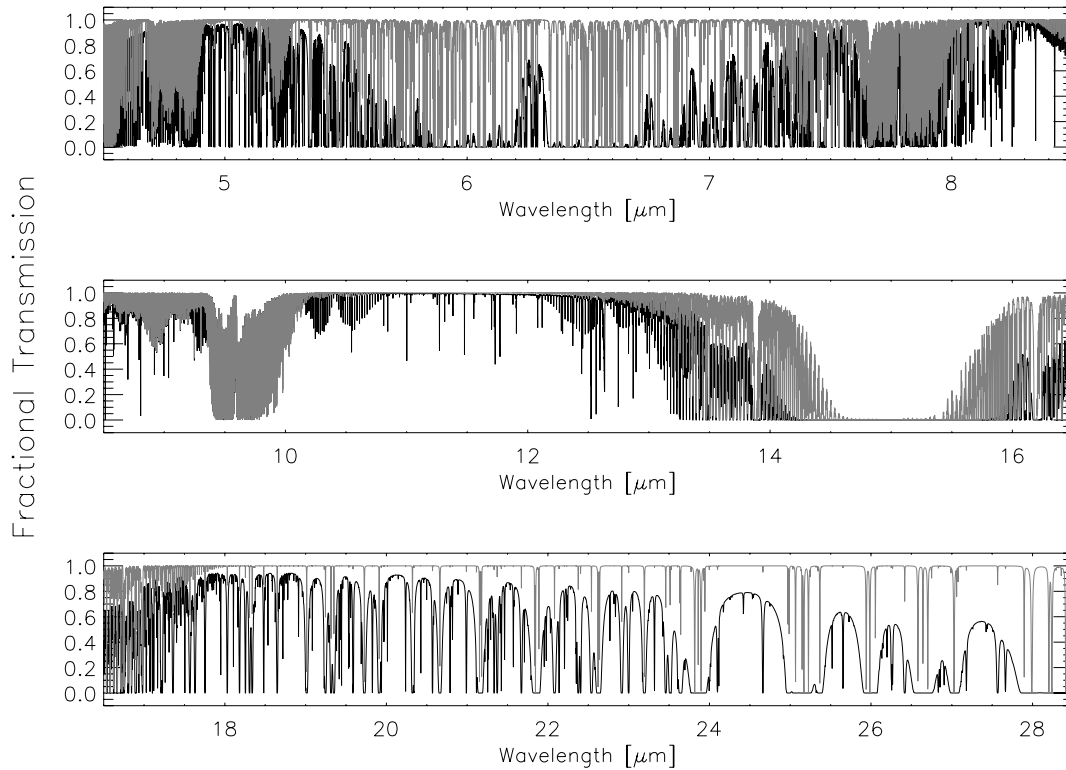


Figure 3. A comparison of the atmospheric transmission across the EXES operating range from Mauna Kea (black) and SOFIA (grey). The greatest improvements in the transparency are seen in regions dominated by water vapor such as the 5-7 μm and 20 μm region.

use of TEXES as a Gemini visitor instrument starting in 2006B will provide us with experience delivering data products to a similar user community.

The quick-look data acquisition software is written in IDL and provides the instrument operator with feedback as each coadded frame is saved to disk. The software can display raw data, background subtracted pairs, or a sum over subtracted pairs. The user can interactively select rows or columns for combining including the option of combining positive and negative beams typical of point sources nodded on the slit. The display can rotate the data so dispersion runs roughly along a displayed row. By summing over dispersion, it is possible to monitor the light through the slit on time scales suitable for hand guiding. The display also creates essentially a “strip chart” of the median value for the raw frames that can be used to monitor background levels. The quick-look will present a simply-constructed, background-subtracted map for the appropriate observing mode.

The data reduction pipeline is written in Fortran and runs on a separate computer from the data acquisition. Before running the data reduction pipeline, the raw data (including appropriate calibration files) must be copied from the instrument data disk. The reduction pipeline can be run interactively or in batch mode. It contains many parameters for dealing with all observing modes. It works best for bright point sources and will produce an optimally extracted, near publishable quality 1D spectrum for these sources within minutes of completing a file and copying it to the appropriate machine. We hope to store both raw and pipeline reduced data with FITS headers in the SOFIA data archive.

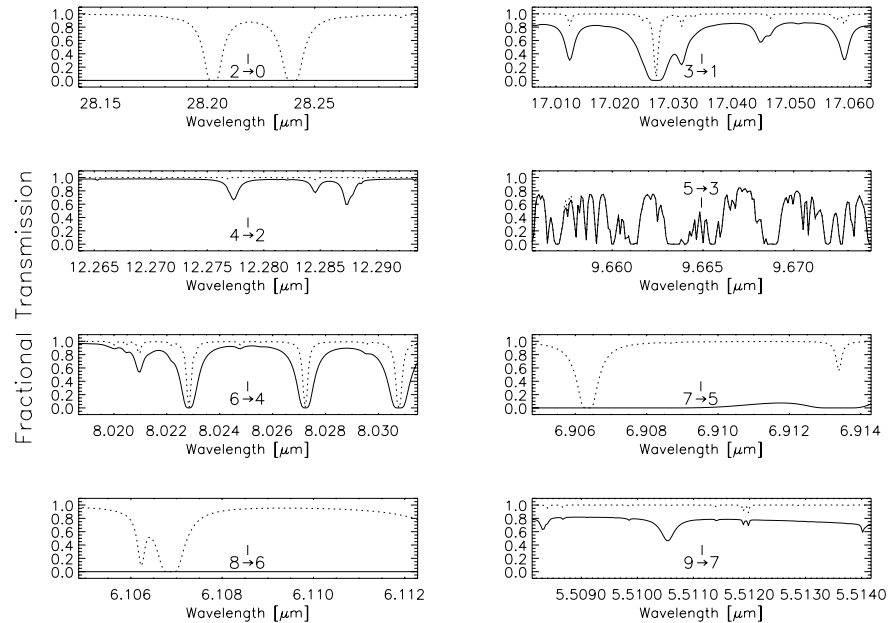


Figure 4. A comparison of the atmospheric transmission from Mauna Kea (solid) and SOFIA (dotted) near H_2 pure rotational transitions. The H_2 transition is marked and identified by the J states involved. While several of these transitions can be observed from the ground, especially with a favorable Doppler shift, the H_2 $J=2\rightarrow 0$, $J=7\rightarrow 5$, and $J=8\rightarrow 6$ transitions are completely unobservable from the ground. The $J=5\rightarrow 3$ transition near $9.665\ \mu\text{m}$ is not improved at all from the airplane, the two curves fall on top of each other, because this line lies within the telluric ozone band.

5. BASIC SCIENCE

We believe potential projects with EXES and SOFIA will concentrate on spectral regions where ground-based MIR observations will be uncompetitive because of the atmosphere. Figure 3 presents typical atmospheric transmission from Mauna Kea and SOFIA over the EXES spectral region. Over much of the MIR, reduced transmission means more than just the absorption of astrophysical photons (reducing the signal), it also means increased background emission (increasing the noise). While the transmission from SOFIA is dramatically improved over much of the range, a significant amount of the $8\text{--}13\ \mu\text{m}$ window has comparable transmission from the ground. When planning an observation, it is important to examine the atmospheric feature at high resolution; some lines, such as the H_2 $v=0$ $J=4\rightarrow 2$ transition at $12.279\ \mu\text{m}$ are near fairly isolated atmospheric features in otherwise clean spectral regions.

H_2 pure rotational lines are one likely target for SOFIA. Although the $J=3\rightarrow 1$, $J=4\rightarrow 2$, and $J=6\rightarrow 4$ lines are all available from the ground, all three lines have better transmission from SOFIA, and the $J=2\rightarrow 0$ and $J=7\rightarrow 5$ lines become possible. While the $J=2\rightarrow 0$ line is the best tracer of the coldest gas, the $J=7\rightarrow 5$ line is an important tracer for warm gas.

Other likely observations using EXES and SOFIA will involve molecular absorption along the line-of-sight to infrared-bright, forming protostars. By observing several J-states of the same vibrational level, this technique allows investigation of the temperature, density, chemistry, dynamics, and optical depth of gas associated with star formation. This mode of study is complementary to radio and millimeter observations of rotational emission: the infrared absorption method samples a consistent column of gas defined by the size of the background source and can search for molecules without dipole transitions, such as CH_4 , CH_3 , and C_2H_2 .

While some molecular transitions are located in spectral regions available from the ground, great improvement will come from EXES on SOFIA. In Figure 5, we compare the atmospheric transmission from Mauna Kea and SOFIA for regions with transitions of H_2O , CH_4 , C_2H_2 , HCN , CH_3 , and SO_2 . These simple molecules play

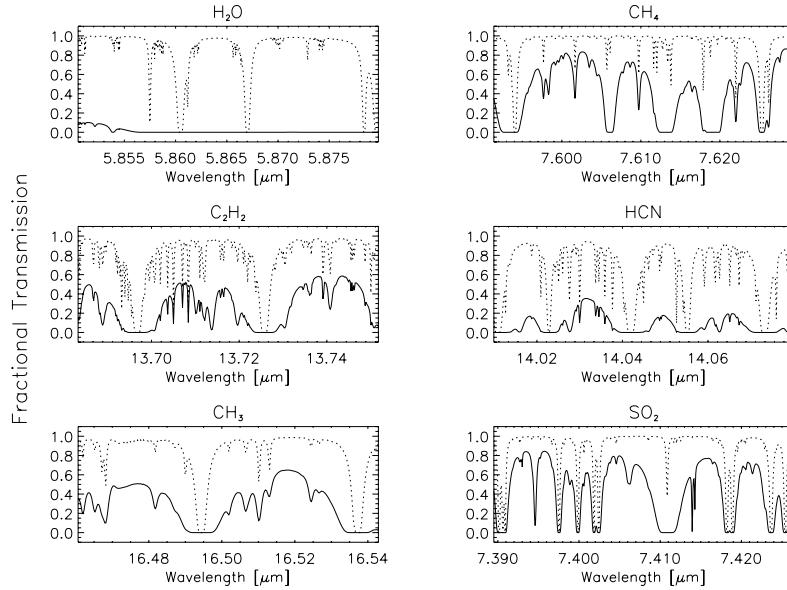


Figure 5. A comparison of the atmospheric transmission from Mauna Kea (solid) and SOFIA (dotted) over slightly less than a single EXES spectral setting. The spectral settings were chosen with a single molecule in mind, as denoted for each panel. These particular settings were chosen to cover a wide range in excitation conditions. The H₂O setting includes 5 lines, the CH₄ includes 4 lines, and the others include more than 10 in all cases. To aid in understanding what is possible, we have made useful observations of targets at both the C₂H₂ and SO₂ settings with TEXES. However, it is often necessary to choose carefully the Doppler shift of the target relative to the instrument to get useful results. For reference, each panel has a width of 1500 km/s.

important roles in the chemistry, heating, and cooling of the ISM. For molecules with significant opacity in our atmosphere, such as H₂O and CH₄, the astronomical source will need to be Doppler shifted to move the transition off the telluric feature. To provide context, we have observed the C₂H₂ and SO₂ settings from the ground on multiple occasions with reasonable results.

Within the solar system, we anticipate EXES on SOFIA being an important tool for the study of relatively tenuous atmospheres where spectral features will be narrow. These features may be in emission, such as from comets and planetary stratospheres, or in absorption against a bright background, such as from the Martian atmosphere and Jupiter's moon, Io. Studies of H₂O, CH₄, and, particularly from comets with large Doppler shifts relative to Earth, CO₂ may all be carried out. These observations will bear on recent reports of Martian CH₄^{9,10}, the interaction of Saturn's rings with its stratosphere,¹¹ and the importance of cometary impacts to the composition of Jupiter's stratosphere.¹²

External to the solar system, EXES and SOFIA will provide observations of star and planet formation regions that will help uncover the physical and chemical properties of these regions. Gas in the inner regions of protoplanetary disks (R<10 AU) has been fairly difficult to constrain although CO ro-vibrational and some hot H₂O and OH observations are important.¹³ For the H₂ rotational lines mentioned above, EXES and SOFIA will achieve similar sensitivity to the *Spitzer Space Telescope* for narrow lines.¹⁴ This will be most significant in sources with any associated dust continuum. EXES will permit observations of ro-vibrational H₂O in the strong 5-7 μm ν₂ band. ISO used these lines to study H₂O absorption along the line of sight toward massive star forming regions,¹⁵ but their application to lower mass disk sources will be impossible because of the instrumental requirements until EXES on SOFIA. For the important question of gas dissipation timescales in more evolved disks, EXES and SOFIA will permit observations of the [S I] line shown to be a strong coolant and a very promising MIR line for detection with *Spitzer*.¹⁶

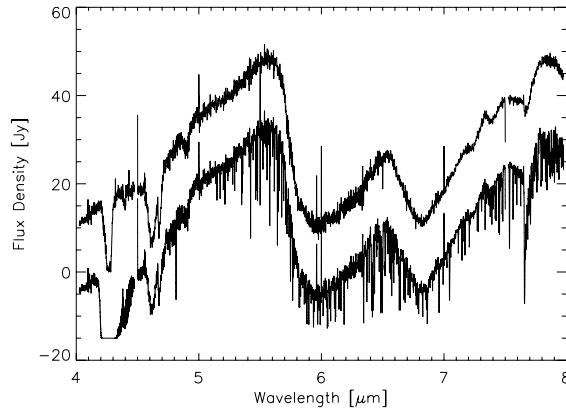


Figure 6. (upper trace) ISO data for W33A.¹ (lower trace) Simulation of the effects of telluric absorption on observations of W33A with SOFIA. The W33A ISO data were multiplied by a model of atmospheric transmission from SOFIA and then convolved to EXES low spectral resolution. The resulting spectrum was then displaced by 15. Eight separate settings would be needed to cover the displayed range.

6. IMPACT OF 1024×1024 DETECTOR

An opportunity exists for EXES to incorporate a 1024×1024 Si:As detector, available on a long-term loan basis. The loan request was made jointly by the SOFIA Project Office and the NASA Ames detector group and approved by NASA Headquarters (Physics and Astronomy Division). A mega-pixel array would represent a factor of 16 more pixels in our focal plane. The mega-pixel array will provide better optical performance leading to increased spectral resolution while also increasing the wavelength coverage of EXES by a factor of 2 to 4. Scientifically, this would make EXES a much better instrument with which to study both solids and gas.

An instrument designed to study both solids and gas is subject to nearly contradictory requirements. Solid molecular features have quite broad widths, pushing instruments toward large spectral coverage. Since information regarding the ice matrix and the presence of relatively minor amounts of complex species are contained within the line profile, moderate spectral resolving power is required to access that information. Gas features are very narrow and require very high spectral resolution both to examine the line profile and to achieve the best sensitivity for weak features. With good spectral coverage, multiple rotational levels can be seen in a single setting allowing a more detailed study of the gas properties and robust detections of trace species. Large wavelength coverage will also allow for serendipitous detections of new molecular species.

As a sub-orbital platform, SOFIA will be able to detect many ice features seen from space.¹⁷ The features found between 4 and 8 μm include CO_2 , $^{13}\text{CO}_2$, OCN^- (“XCN”), CO , H_2CO , HCOOH , H_2O , CH_3OH , and CH_4 . While the residual atmosphere above SOFIA will affect the observation of these ices (6), the broad nature of the features, especially when compared with the narrow residual telluric features, will make telluric corrections quite effective. The effects of the atmosphere are actually similar to ground-based observations in parts of the H band (1.48 to 1.78 μm) where features broader than the atmospheric lines are readily recovered after dividing the target spectrum by a hot star spectrum.¹⁸

Putting 16 times the pixels into the EXES focal plane will permit two fundamental changes to the system. We currently use focal reducing optics in front of the detector to set the final f /ratio so that we are Nyquist sampling the diffraction pattern and fitting complete orders on the detector at $\lambda = 10 \mu\text{m}$. Below 10 μm , we do not Nyquist sample the diffraction pattern, thus losing some information. Beyond 10 μm , the orders are larger than the 256×256 pixel detector resulting in gaps in the extracted spectra. The focal reducing optics cause light loss at the two refractive surfaces, but give adequate performance over the detector array. With the 1024×1024 pixel detector, we can remove the focal reducing optics. This will improve the transmission and the optical performance, while pushing Nyquist sampling of the diffraction pattern down to 5 μm and complete coverage of

orders (no gaps) out to $\lambda = 20 \mu\text{m}$. We are confident this will allow us to improve the EXES spectral resolution by as much as a factor of 2 to $R = 200,000$ at $5 \mu\text{m}$ and give more “usable” resolution at all wavelengths due to the increased sampling. The new detector will also fill the focal plane and give at least twice as much spectral coverage in all spectral modes.

Removing the focal reducer will also affect our background photon rate. With our current array, we routinely achieve background-limited performance in our high resolution mode. At lower resolutions, where the photon flux is higher, the detector performance is hampered by irregular spikes on random pixels. We do not know if this is a common feature of these types of arrays or specific to the 256×256 pixel detector we use. We have tied the behavior to the bias across the detector and so guess we are seeing a charge avalanche. The net effect of this behavior is to hurt our sensitivity and prevent us from reaching background-limited performance. With the slower f/number beam that comes without the focal reducing optics, the effective size on the sky of each pixel is reduced. The background photon rate goes as the inverse square of the effective size on the sky. Therefore, we anticipate lower photon rates with the larger array and hope to avoid the spiking that currently prevents us from reaching background-limited performance in all spectroscopic modes.

Implementation of the mega-pixel array still requires funds for purchasing suitable electronics and the additional testing required to debug the system. We are hopeful that these relatively modest funds will be available sometime in the future.

ACKNOWLEDGMENTS

Design and construction of EXES is made possible with grants from the Universities Space Research Association: USRA 8500-98-008 and USRA 8500-03-101.

REFERENCES

1. E. L. Gibb, D. C. B. Whittet, W. A. Schutte, A. C. A. Boogert, J. E. Chiar, P. Ehrenfreund, P. A. Gerakines, J. V. Keane, A. G. G. M. Tielens, E. F. van Dishoeck, and O. Kerkhof, “An Inventory of Interstellar Ices toward the Embedded Protostar W33A,” *Astrophysical Journal* **536**, pp. 347–356, June 2000.
2. E. Becklin, “SOFIA: Stratospheric Observatory for Infrared Astronomy,” in *IAU Symposium*, D. C. Lis, G. A. Blake, and E. Herbst, eds., pp. 9–+, Aug. 2005.
3. E. F. Erickson, “The SOFIA program,” in *The Dusty and Molecular Universe: A Prelude to Herschel and ALMA*, A. Wilson, ed., pp. 69–74, Jan. 2005.
4. J. H. Lacy, M. J. Richter, T. K. Greathouse, D. T. Jaffe, and Q. Zhu, “TEXES: A Sensitive High-Resolution Grating Spectrograph for the Mid-Infrared,” *Publications of the ASP* **114**, pp. 153–168, Feb. 2002.
5. M. J. Richter, J. H. Lacy, D. T. Jaffe, M. K. Hemenway, and W. Yu, “EXES: an echelon cross echelle spectrograph for SOFIA,” in *Proc. SPIE Vol. 3354, p. 962-972, Infrared Astronomical Instrumentation, Albert M. Fowler; Ed.*, **3354**, pp. 962–972, Aug. 1998.
6. M. J. Richter, J. H. Lacy, D. T. Jaffe, T. K. Greathouse, and M. K. Hemenway, “EXES: a progress report on the development of a high-resolution mid-infrared grating spectrograph for SOFIA,” in *Proc. SPIE Vol. 4014, p. 54-64, Airborne Telescope Systems, Ramsey K. Melugin; Hans-Peter Roeser; Eds.*, **4014**, pp. 54–64, June 2000.
7. K. G. Bach, B. W. Bach, and B. W. Bach, “Large-ruled monolithic echelle gratings,” in *Proc. SPIE Vol. 4014, p. 118-124, Airborne Telescope Systems, Ramsey K. Melugin; Hans-Peter Roeser; Eds.*, **4014**, pp. 118–124, June 2000.
8. G. G. Fazio, J. L. Hora, L. E. Allen, M. L. N. Ashby, P. Barmby, L. K. Deutsch, J.-S. Huang, S. Kleiner, M. Marengo, S. T. Megeath, G. J. Melnick, M. A. Pahre, B. M. Patten, J. Polizotti, H. A. Smith, R. S. Taylor, Z. Wang, S. P. Willner, W. F. Hoffmann, J. L. Pipher, W. J. Forrest, C. W. McMurty, C. R. McCreight, M. E. McKelvey, R. E. McMurray, D. G. Koch, S. H. Moseley, R. G. Arendt, J. E. Mentzell, C. T. Marx, P. Losch, P. Mayman, W. Eichhorn, D. Krebs, M. Jhabvala, D. Y. Gezari, D. J. Fixsen, J. Flores, K. Shakoorzadeh, R. Jungo, C. Hakun, L. Workman, G. Karpati, R. Kichak, R. Whitley, S. Mann, E. V. Tollestrup, P. Eisenhardt, D. Stern, V. Gorjian, B. Bhattacharya, S. Carey, B. O. Nelson, W. J. Glaccum, M. Lacy, P. J. Lowrance, S. Laine, W. T. Reach, J. A. Stauffer, J. A. Surace, G. Wilson, E. L. Wright,

- A. Hoffman, G. Domingo, and M. Cohen, "The Infrared Array Camera (IRAC) for the Spitzer Space Telescope," *Astrophysical Journal Supplement Series* **154**, pp. 10–17, Sept. 2004.
9. V. A. Krasnopolsky, J. P. Maillard, and T. C. Owen, "Detection of methane in the martian atmosphere: evidence for life?," *Icarus* **172**, pp. 537–547, Dec. 2004.
 10. V. Formisano, S. Atreya, T. Encrenaz, N. Ignatiev, and M. Giuranna, "Detection of Methane in the Atmosphere of Mars," *Science* **306**, pp. 1758–1761, Dec. 2004.
 11. J. G. Luhmann, R. E. Johnson, R. L. Tokar, S. A. Ledvina, and T. E. Cravens, "A model of the ionosphere of Saturn's rings and its implications," *Icarus* **181**, pp. 465–474, Apr. 2006.
 12. E. Lellouch, B. Bézard, J. I. Moses, G. R. Davis, P. Drossart, H. Feuchtgruber, E. A. Bergin, R. Moreno, and T. Encrenaz, "The Origin of Water Vapor and Carbon Dioxide in Jupiter's Stratosphere," *Icarus* **159**, pp. 112–131, Sept. 2002.
 13. J. Najita, J. Carr, A. Glassgold, and J. Valenti, "Gaseous Inner Disks," in *Protostars and Planets V*, B. Reipurth, D. Jewitt, and K. Keil, eds., pp. 16–+, Oct. 2006.
 14. D. Hollenbach, U. Gorti, M. Meyer, J. S. Kim, P. Morris, J. Najita, I. Pascucci, J. Carpenter, J. Rodmann, T. Brooke, L. Hillenbrand, E. Mamajek, D. Padgett, D. Soderblom, S. Wolf, and J. Lunine, "Formation and Evolution of Planetary Systems: Upper Limits to the Gas Mass in HD 105," *Astrophysical Journal* **631**, pp. 1180–1190, Oct. 2005.
 15. A. M. S. Boonman and E. F. van Dishoeck, "Abundant gas-phase H₂O in absorption toward massive protostars," *Astronomy and Astrophysics* **403**, pp. 1003–1010, June 2003.
 16. U. Gorti and D. Hollenbach, "Models of Chemistry, Thermal Balance, and Infrared Spectra from Intermediate-Aged Disks around G and K Stars," *Astrophysical Journal* **613**, pp. 424–447, Sept. 2004.
 17. P. Ehrenfreund and W. A. Schutte, "Infrared Observations of Interstellar Ices," in *Astrochemistry: From Molecular Clouds to Planetary*, Y. C. Minh and E. F. van Dishoeck, eds., pp. 135–+, 2000.
 18. W. D. Vacca, M. C. Cushing, and J. T. Rayner, "A Method of Correcting Near-Infrared Spectra for Telluric Absorption," *Publications of the ASP* **115**, pp. 389–409, Mar. 2003.